Funded by
the European Union

This article has been submitted to ICEMES 2023

Hyperspectral Image Visualization Based on Maximum-Reflectance Wavelength Colorization

Kamal Marandskiy[1] and Mihai Ivanovici[2]

Electronics and Computers Department
Transilvania University of Brașov, Brașov, Romania

[1]kamal.marandskiy@unitbv.ro, [2]mihai.ivanovici@unitbv.ro

Abstract

Hyperspectral imaging is an important part of remote sensing technologies, providing detailed spectral information about the observed scene. Visualization of the resulting hyperspectral data cube is a challenge due to the large number of available spectral bands. In this paper, we propose a visualization technique that is based on mapping the corresponding RGB triplet to the wavelength value with the maximum reflectance. The approach is based on the assumption that the wavelength with maximum reflectance may reveal useful information about the objects and materials in the scene. We show experimental results on the widely-known Pavia University hyperspectral image. We interpret the results, provide a comparison with the existing methods and perform a quantitative evaluation for proving the usefulness of the proposed approach.

1 Introduction

Hyperspectral images (HSIs) are captured over a wide range of the electromagnetic spectrum providing detailed information about the Earth's surface. Hyperspectral images have hundreds of spectral channels that cover visible and infrared spectra; thus, they are an important source of information due to remote sensing technologies [1], [2]. Due to this ability, hyperspectral imaging applications have been developed for solving practical problems such as object detection [3], object recognition [4], identifying farming issues (weeds, nutrient deficiency, diseases) [5], etc. However, effectively visualizing hyperspectral images is a challenge since displays are designed to show one or three bands. Many approaches for visualizing HSIs have been proposed. Hence, HSI visualization methods can be divided into 2 main categories, i.e., the band selection-based and transform-based methods [6]. According to the reference [7], visualization approaches can be classified into 3 categories: band selection-based methods, transform-based methods, and fusion-based methods. However, in reference [8], authors classified proposed approaches into 5 different categories namely: band selection, principal component analysis (PCA) -based approaches, linear approaches, approaches based on digital image processing techniques, and machine/deep learning methods.

Band selection consists of choosing the 3 optimal bands that contain full information about the scene, each band representing red, green, and blue channels, accordingly. Commercial geospatial image analysis software products such as ENVI [9] gives the opportunity to the user to visualize hyperspectral images by manually selecting 3 bands as color channels. More complicated unsupervised band selection approaches have been developed based on one-bit transform (1BT) [10]. Decolorization-based hyperspectral image visualization (DHV) process has three steps: chromaticity transformation, saliency map generation, and color restoration. The method separates color information from luminance information, then restores color to the grayscale image for contrast enhancement by selecting the spectral bands which contain the most information about the scene [11]. In [8], authors propose linear and non-linear visualization methods for hyperspectral images, evaluating their impact on the amount of information and complexity of a scene. The linear method emulates a consumer-grade digital camera sensor (Canon 5D Mark II) while the non-linear method uses an Artificial Neural Network (ANN) trained on a 24-sample color checker. Another proposed approach is a color matching function (CMF)-based that maps the hyperspectral data onto a displayable color space in three steps: selecting the appropriate CMF, normalizing the data, and mapping it to a color space [12]. Constrained manifold learning for hyperspectral imagery visualization (CML) is another approach for visualizing the HSIs that preserves spectral and spatial data. The semi-supervised locally linear embedding technique is employed to map high-dimensional data to a lower-dimensional manifold and it allows the user to define the constraints [13]. On the other hand, the main idea of transform-based methods is to represent the important information of the original image through a spectral transformation method. Examples of this approach are PCA for dimension reduction of the data, a visualization technique to map the three principal components to the R, G, and B channels of the color image [14], another technique independent component analysis (ICA), and it is a frequently used unsupervised classification method [15]. Basic idea is to decompose a set of multivariate signals into a base of statistically-independent signals with minimal loss of information content. There are many ICA algorithms that have been developed, the well-known one is FastICA with kurtosis maximization [16], [17].

In this article, we propose a visualization technique based on mapping RGB triplets to the wavelength values with the maximum reflectance in the spectral reflectance curve of each pixel. Various surface types like water, bare soil and vegetation reflect radiation differently in various channels, thus we make the assumption that the maximum-reflectance wavelength of a pixel spectral signature may offer useful information about the objects and materials in the acquired scene. The proposed pixel-wise technique has the advantage of being very simple while emphasizing the most reflective band in every pixel. The disadvantage is the fact that only one spectral band is used for visualization and this spectral band differs for each pixel.

The rest of this paper is organized as follows. The proposed HSI visualization technique is described in Section II and the experimental results are presented in Section III, along with a comparison with state-of-the-art techniques. Finally, conclusions are provided in Section IV.

2 Proposed Method

The proposed approach consists of two steps: (i) determining the maximum reflectance value in a pixel spectral signature and the corresponding wavelength; and (ii) assigning an RGB triplet to each previously-determined wavelength, thus realizing the visualization of the hyperspectral data through the colorization of the maximum-reflectance wavelength. The implementation of the proposed approach was done in Matlab. The two steps are described and illustrated in what follows.

2.1 Determining the maximum reflectance and the corresponding wavelength (λ)

For each pixel, we determine the wavelength value of the maximum reflectance in the spectral reflectance curve. This step is illustrated in Fig. 1, where the maximum reflectance corresponds to the wavelength of 734 nm.

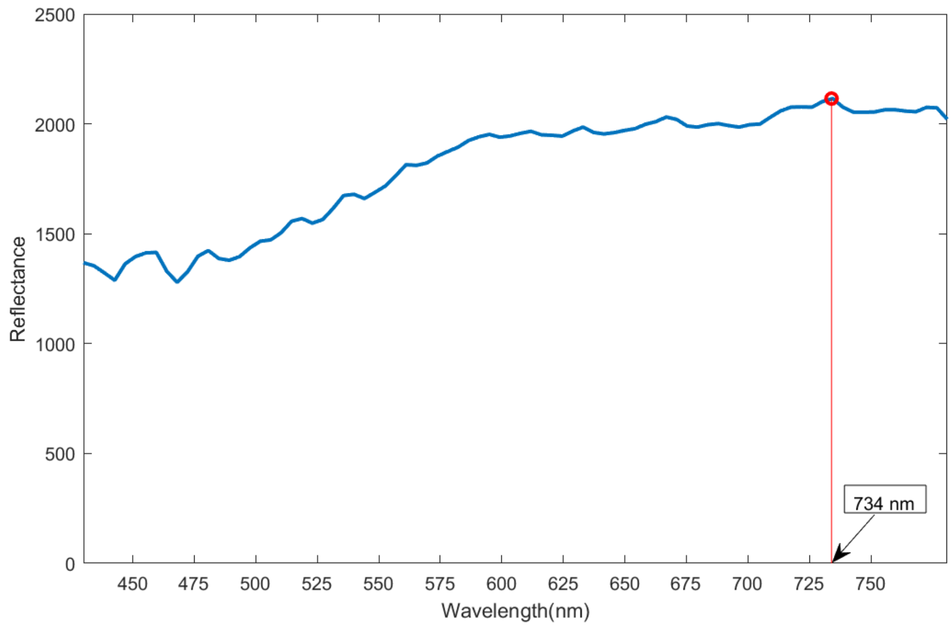

Figure 1: A pixel spectral signature of Pavia University hyperspectral image and its maximum reflectance.

2.2 Assigning the corresponding RGB triplet to the maximum-reflectance wavelength

For the conversion of wavelength to RGB color space we used the approach in [18]. The RGB color components are computed as piece-wise linear functions of the wavelength λ. The functions used to assign each color channel value in the RGB triplet are depicted in Fig. 2. For implementing the conversion step we used the look-up tables available in [19], resulting in a faster run of the proposed approach.

The resulting colors as a function of wavelength (λ) are depicted in Fig. 3.

3 Experiments

The Pavia University hyperspectral data set was deployed in our experiments [20]. The hyperspectral data cube was captured with a Reflective Optics System Imaging Spectrometer (ROSIS) sensor and has a spatial resolution of 610×340 pixels and 103 spectral bands, thus resulting in a $610\times340\times103$ size

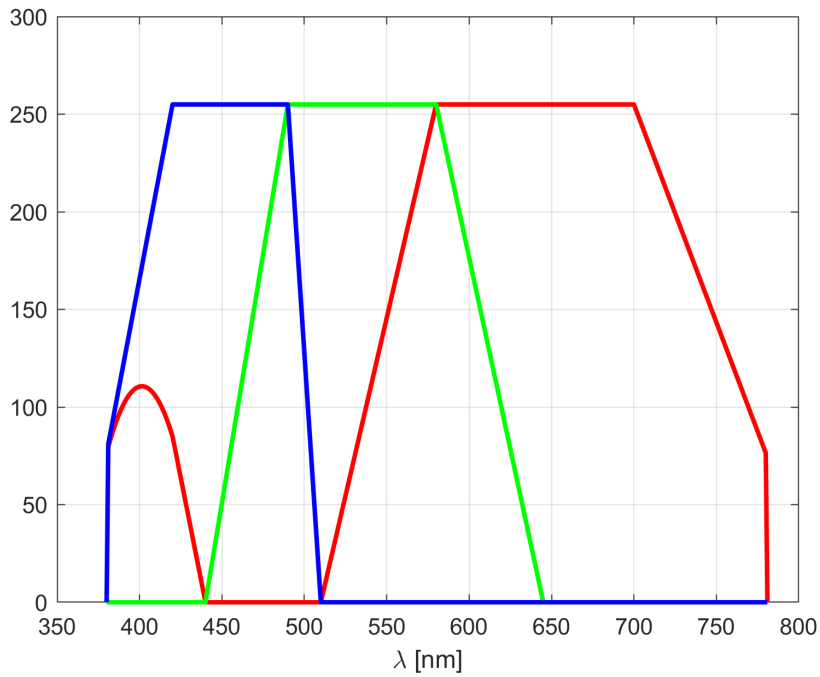

Figure 2: The functions used for the conversion of wavelength to RGB, for the red, green and blue components.

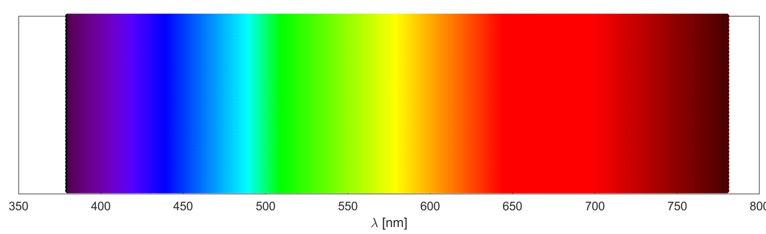

Figure 3: The colors in the visible spectrum, as a function of wavelength (λ).

data cube. The sensor captures a range from 430 to 860 nm and bandwidth is equivalent to 4 nm for all 103 spectral bands. We disregarded the number of bands from the upper end of the acquired spectrum since they are in the infrared range. Only visible spectral bands were considered for colorization through the mapping of the RGB values. In this case, the considered Pavia University hyperspectral cube has dimensions of $610 \times 340 \times 84$.

In Fig. 4 we present the experimental results obtained on two crops of the Pavia University data set. We depict the visualization results, as well as the gray-scale pseudo-image of maximum reflectance wavelength (denoted λ pseudo image).

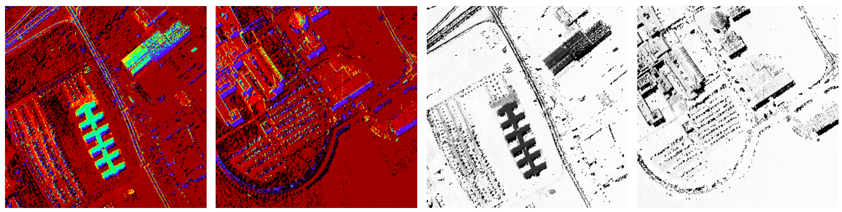

(a) RGB image upper part (b) RGB image lower part (c) λ pseudo image upper part (d) λ pseudo image lower part

Figure 4: Experimental results of the proposed approach on Pavia University image crops.

One can notice that the visualization result exhibits a lot of red shades, as a consequence that of the presence of mainly natural materials in the scene: bare soil, meadows, gravel, and trees. The artificial surfaces (asphalt, painted metal sheets) are depicted with bluish colors (Fig. 4(a) and Fig. 4(b). For the painted metal sheets, the proposed method shows that the maximum-reflectance wavelength is the one determining the perceived color in the visualization aiming at producing the natural colors in the scene. Another particular aspect is the fact that the shadows are emphasized, being colorized with a dark blue/violet color.

In Fig. 5 we show the comparison of the proposed approach with other visualization techniques. Fig. 5(a) represents the result of our proposed method for the visualization of HSI. Fig. 5(b) is the 2D matrix constructed from wavelength values of maximum reflectance and a pseudo image containing features of the actual dataset. Fig. 5(c) and Fig. 5(d) are the results of experiments with the linear color formation (based on the Canon 5D camera sensitivity curves) and ANN respectively. Fig. 5(e) is based on CMF while Fig. 5(f) was constructed by the CML technique. Fig. 5(g) shows the Pavia University scene which was visualized with the PCA method and Fig. 5(h) shows the one that was accomplished with DHV. Finally, Fig. 5(i) is the result of the Quality-Based Band Selection (QBS) method [21]. One can observe that the Lin, ANN, CMF and CML methods aim at reproducing the natural color of the scene, as perceived by an observer. The PCA, DHV, and QBS aim to represent the scene in a different representation space, in order to emphasize other properties of the spectral reflectance curves, like the highest information and variability components (PCA) or the highest-quality bands (QBS).

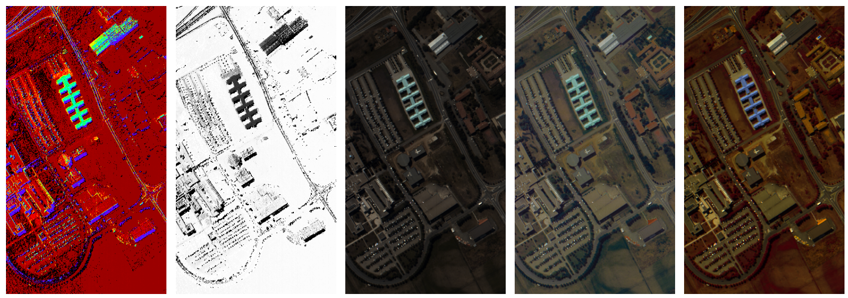

(a) Proposed method (b) λ pseudo image (c) Lin (d) ANN (e) CMF

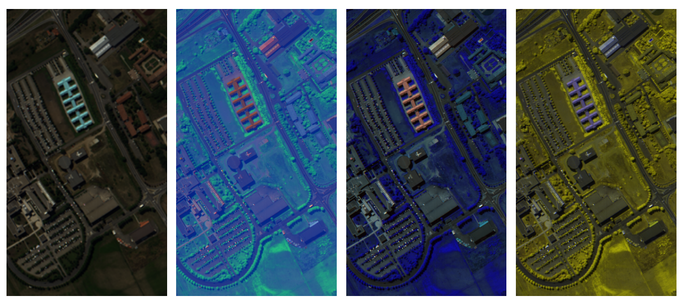

(f) CML (g) PCA (h) DHV (i) QBS

Figure 5: Comparison of the proposed approach with state-of-the-art visualization techniques.

Despite being a visualization technique, the proposed approach shows the potential in pixel classification and, thus, image segmentation of the hyperspectral data. In what follows, we performed a quantitative evaluation of the proposed approach's capabilities of correctly classifying pixels belonging to several classes of materials present in the Pavia University scene. In order to evaluate the results we used the available ground truth information [20]. We observed that shadows appear as violet, painted metal sheets as cyan while natural surfaces (meadows, trees, bare soil, etc.) appear as red. Thus, we used labeled samples in the ground truth data set to compute the percentage of correctly identified pixels in the proposed method. The evaluation was applied to a total of 5 samples: meadows, trees, painted metal sheets, bare soil, and shadows. Meadows, trees, and bare soil were considered natural surfaces while painted metal sheets were an example of artificial surfaces. We considered shadows as a separate category. Table 1 represents the results of the evaluation. For the considered categories, we show the corresponding wavelength range and the percentage of correctly-classified pixels (denoted as PCCP). Results indicate that the approach has the ability to classify the different materials on the scene with very high accuracy.

Table 1: QUANTITATIVE EVALUATION OF CORRECTLY-CLASSIFIED PIXELS.

Samples	Painted metal sheets	Shadows	Natural surfaces
Range (λ)	$470 - 550\ nm$	$430 - 470\ nm$	$620 - 780\ nm$
PCCP	99.5 %	94.2 %	99.8 %

4 Conclusion

Visualization of the hyperspectral data cubes is a challenge due to the high number of spectral bands. Various approaches exist that consider all or a certain subset of the available spectral bands. In this paper, we proposed a visualization technique that is based on mapping the corresponding RGB triplet to the wavelength value with the maximum reflectance in the spectral reflectance curve of each pixel. The approach has two steps: determine the wavelength value where the reflectance is at its maximum in each pixel, then map the RGB triplet to the corresponding wavelength value. The proposed pixel-wise method for visualization consequently uses only one spectral band from the data cube. We showed experimental results on a real hyperspectral image and its comparison with other methods. Results indicated that our approach is able to emphasize surfaces of similar nature in the hyperspectral image, mainly the artificial and natural materials, as well as shadows which are important to detect in remote sensing applications. The shadows are represented with violet, indicating that the wavelength corresponding to the blue-violet has the highest reflectance, regardless of the fact that the underlying material is natural. We performed a quantitative evaluation by computing the percentage of correctly-classified pixels, based on the available ground truth, for three types of surfaces: shadows, metal sheets, and natural. We conclude that, unlike other methods, the proposed approach has usefulness in hyperspectral image visualization and pixel classification scenarios, for emphasizing surfaces of similar kind or nature.

Acknowledgments

Funded by the European Union. The AI4AGRI project entitled "Romanian Excellence Center on Artificial Intelligence on Earth Observation Data for Agriculture" received funding from the European Union's Horizon Europe research and innovation program under grant agreement no. 101079136. Views and opinions expressed are however those of the author(s) only and do not necessarily reflect those of the European Union. Neither the European Union nor the granting authority can be held responsible for them

Funded by
the European Union

References

[1] M. J. Khan, H. S. Khan, A. Yousaf, K. Khurshid, and A. Abbas, "Modern trends in hyperspectral image analysis: A review," *Ieee Access*, vol. 6, pp. 14118–14129, 2018.

[2] Y. Gu, T. Liu, X. Jia, J. A. Benediktsson, and J. Chanussot, "Nonlinear multiple kernel learning with multiple-structure-element extended morphological profiles for hyperspectral image classification," *IEEE Transactions on Geoscience and Remote Sensing*, vol. 54, no. 6, pp. 3235–3247, 2016.

[3] Y. Xu, Z. Wu, J. Chanussot, M. Dalla Mura, A. L. Bertozzi, and Z. Wei, "Low-rank decomposition and total variation regularization of hyperspectral video sequences," *IEEE Transactions on Geoscience and Remote Sensing*, vol. 56, no. 3, pp. 1680–1694, 2017.

[4] X. Kang, S. Li, L. Fang, and J. A. Benediktsson, "Intrinsic image decomposition for feature extraction of hyperspectral images," *IEEE Transactions on Geoscience and Remote Sensing*, vol. 53, no. 4, pp. 2241–2253, 2014.

[5] B. Lu, P. D. Dao, J. Liu, Y. He, and J. Shang, "Recent advances of hyperspectral imaging technology and applications in agriculture," *Remote Sensing*, vol. 12, no. 16, p. 2659, 2020.

[6] X. Kang, P. Duan, S. Li, and J. A. Benediktsson, “Decolorization-based hyperspectral image visualization,” *IEEE Transactions on Geoscience and Remote Sensing*, vol. 56, no. 8, pp. 4346–4360, 2018.

[7] P. Duan, X. Kang, S. Li, and P. Ghamisi, “Multichannel pulse-coupled neural network-based hyperspectral image visualization,” *IEEE Transactions on Geoscience and Remote Sensing*, vol. 58, no. 4, pp. 2444–2456, 2019.

[8] R.-M. Coliban, M. Marincaş, C. Hatfaludi, and M. Ivanovici, “Linear and non-linear models for remotely-sensed hyperspectral image visualization,” *Remote Sensing*, vol. 12, no. 15, p. 2479, 2020.

[9] L. GEOSPATIAL, “Envi software.”

[10] B. Demir, A. Celebi, and S. Erturk, “A low-complexity approach for the color display of hyperspectral remote-sensing images using one-bit-transform-based band selection,” *IEEE Transactions on Geoscience and Remote Sensing*, vol. 47, no. 1, pp. 97–105, 2008.

[11] X. Kang, P. Duan, S. Li, and J. A. Benediktsson, “Decolorization-based hyperspectral image visualization,” *IEEE Transactions on Geoscience and Remote Sensing*, vol. 56, no. 8, pp. 4346–4360, 2018.

[12] N. P. Jacobson and M. R. Gupta, “Design goals and solutions for display of hyperspectral images,” *IEEE Transactions on Geoscience and Remote Sensing*, vol. 43, no. 11, pp. 2684–2692, 2005.

[13] D. Liao, Y. Qian, and Y. Y. Tang, “Constrained manifold learning for hyperspectral imagery visualization,” *IEEE Journal of Selected Topics in Applied Earth Observations and Remote Sensing*, vol. 11, no. 4, pp. 1213–1226, 2017.

[14] J. S. Tyo, A. Konsolakis, D. I. Diersen, and R. C. Olsen, “Principal-components-based display strategy for spectral imagery,” *IEEE Transactions on Geoscience and Remote Sensing*, vol. 41, no. 3, pp. 708–718, 2003.

[15] A. Hyvärinen, J. Karhunen, and E. Oja, “Independent component analysis; a wiley-interscience publication,” 2001.

[16] A. Hyvarinen, “Fast and robust fixed-point algorithms for independent component analysis,” *IEEE transactions on Neural Networks*, vol. 10, no. 3, pp. 626–634, 1999.

[17] Q. Du, N. Raksuntorn, S. Cai, and R. J. Moorhead, “Color display for hyperspectral imagery,” *IEEE Transactions on Geoscience and Remote Sensing*, vol. 46, no. 6, pp. 1858–1866, 2008.

[18] D. Miha and E. Strajescu, “From wavelength to r g b filter,” *University” Politehnica” of Bucharest Scientific Bulletin, Series D: Mechanical Engineering*, vol. 69, no. 2, pp. 77–84, 2007.

[19] “Conversion longueur d’onde - rgb.”

[20] M. Graña, M. Veganzons, and B. Ayerdi, “Hyperspectral remote sensing scenes.”

[21] R.-M. Coliban and M. Ivanovici, “Quality-based band selection for hyperspectral image visualization,” *Remote Sensing Letters*, vol. 14, no. 3, pp. 209–220, 2023.